RESEARCH ARTICLE



ENSO and Paraná flow variability: Long-term changes in their connectivity

Andrés Antico¹ •



| Mathias Vuille² |

¹Institute of Humanities and Social Sciences of the Littoral, National Scientific and Technical Research Council, National University of the Littoral, Santa Fe, Santa Fe, Argentina

²Department of Atmospheric and Environmental Sciences, University at Albany, Albany, New York, USA

Correspondence

Andrés Antico, Institute of Humanities and Social Sciences of the Littoral. CONICET-UNL, Santa Fe, Santa Fe 3000, Argentina.

Email: aantico@santafe-conicet.gov.ar

Funding information

US-NSF award OISE-1743738

Abstract

The Paraná River of South America is one of the largest rivers in the world. Although the connection between Paraná streamflow and El Niño-Southern Oscillation (ENSO) has been studied before, little is known about the longterm (interdecadal) changes of this connectivity. Here we reveal these changes by analysing long instrumental records of Paraná flow, ENSO indices and other climate variables. We find that flow and ENSO were connected in 1876-1940 and 1983-2016, but disconnected in 1941-1982. Flow variability was more related to central Pacific ENSO fluctuations in 1876-1940 but more linked with eastern Pacific ones in 1983-2016, probably because the ENSO-Paraná basin teleconnection was different in the two periods. ENSO-related Pacific climate anomalies exhibited their smallest amplitudes during the disconnection period 1941-1982, suggesting that the ENSO-flow link vanishes when ENSO is weak. We also find that the ENSO-flow disconnection coincided with the coldest phase of the Interdecadal Pacific Oscillation (IPO) in the study period. Thus, the IPO may be modulating the ENSO-flow connectivity. Interestingly, during the disconnection years (1941-1982), flow was related to climate variability observed in sectors of the southern South Atlantic and tropical North Atlantic oceans. This and the other empirical results presented here provide new insights into the Paraná response to ENSO and thus provide valuable information for future mechanistic studies on this response.

KEYWORDS

ENSO, IPO, Paraná River, South America, streamflow

INTRODUCTION 1

The Paraná River streamflow is the third largest in South America (after the Amazon and Orinoco flows), and one of the largest in the world (Schumm and Winkley, 1994). Furthermore, the Paraná basin covers a vast surface area in southeastern South America (SESA) that equals about 60% of the European Union area (see basin location in Figure 1). In SESA, the massive Paraná constitutes an important water way, a major source of hydropower (especially in southern

Brazil), and a vital water resource (UNESCO, 2007). Occasionally, floods caused by extreme Paraná flows have devastating socioeconomic consequences in SESA (Anderson et al., 1993). Because of these important scientific, social and economic aspects of the Paraná River, a large number of studies analysed the variability of its flow (e.g., Amarasekera et al., 1997; Robertson and Mechoso, 1998; Camilloni and Barros, 2000, 2003; Dettinger and Diaz, 2000; Grimm et al., 2000; Labat et al., 2005; Pasquini and Depetris, 2010; Antico et al., 2014; 2016; Silva et al., 2017; Lee et al., 2018;

Montroull et al., 2018; Antico and Diaz, 2020; Abou Rafee et al., 2022, among others). Many of these studies revealed that the Paraná flow variability is related to El Niño-Southern Oscillation (ENSO) in a manner that large and low flows tend to coincide with El Niño and La Niña events, respectively (during El Niño events, spring precipitation increases in the Paraná basin because baroclinic activity is enhanced by a stronger subtropical jet stream; see Garreaud et al., 2009, and references therein). However, only few authors reported long-term (interdecadal) changes in the ENSO-Paraná link (e.g., Labat et al., 2005), and they neither interpreted these changes nor considered pre-1900 instrumental hydroclimate observations in their analyses. This illustrates the current need for a better understanding of many aspects of the ENSO influences on the climate of South America. As stressed by Cai et al. (2020), to fulfil this need it is important to extend back in time the actual observation-based studies of South American climate variability. Hence, here we analyse a recently rescued 1876-2016 Paraná flow record and other observational datasets in order to improve the current knowledge on long-term changes in ENSO-Paraná flow connectivity.

The rest of this paper is organized as follows. Section 2 describes the data and methods used in this work. Next, section 3 presents, discusses and interprets the observed long-term changes of the ENSO-Paraná flow connection. Finally, section 4 presents the conclusions of this study.

2 | DATA AND METHODS

Recently, Antico et al. (2018, 2020) made available records of monthly mean Paraná flow observed at

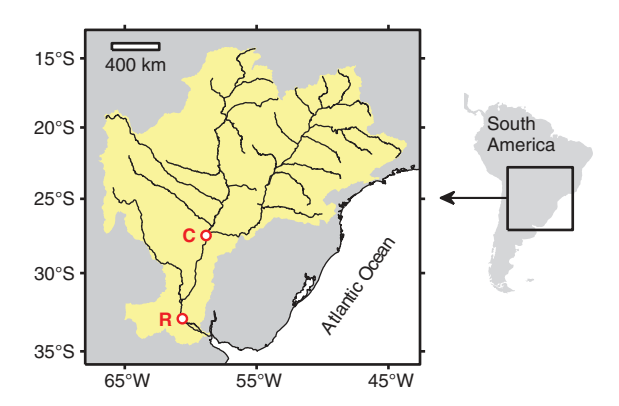


FIGURE 1 Location map of the Paraná River basin (highlighted area). Inside this basin, black lines depict the drainage system. The locations of Rosario (R) and Corrientes (C) cities are indicated by the open circles; both are in Argentina. The basin boundary shown in this figure and used in this study is from GRDC (2020) [Colour figure can be viewed at wileyonlinelibrary.com]

Rosario City (32°57′S, 60°38′W) covering the period 1875–2017. These records are complete (no missing values) and were subjected to quality and homogeneity tests (see Antico *et al.*, 2018, 2020, for descriptions of these tests and of the history of Rosario gauges). Moreover, these flow data were corrected for the gradual gauge sinkings that occurred in 1875–1908 (see Antico *et al.*, 2018, 2020). Since Rosario is relatively close to the river mouth (see Figure 1), flow data from this city reflect changes in runoff integrated over most of the Paraná basin.

The 1875–2006 record of monthly precipitation observed at Corrientes City (27°29′S, 58°50′W) was also used here and it was obtained from the quality-controlled dataset provided by the NOAA Global Historical Climatology Network (version 2) (Vose *et al.*, 1992). This rainfall time series contains 27 missing values (2% of the record length) and no filling procedure was used in this study. It is the only available instrumental precipitation record that goes back to 1875 in the central part of the Paraná basin, far (>500 km) from the river mouth (see Corrientes City location in Figure 1).

To characterize the time evolution of ENSO, we considered two widely used indices: (a) the Niño 3.4 index (N3.4), which is the sea surface temperature (SST) averaged over the El Niño region 3.4 (5°N-5°S, 170°-120°W), and (b) the Southern Oscillation Index (SOI), which is the normalized sea level pressure (SLP) difference between Tahiti and Darwin, Australia, Note that while N3.4 is an oceanic index, SOI is an atmospheric one. Whereas positive (negative) values of N3.4 correspond to El Niño (La Niña) events, positive (negative) SOI values are associated with La Niña (El Niño) episodes. To facilitate the comparison of these two ENSO indices, the sign of the original SOI values was reversed in this study. Zonal asymmetries of ENSO events are taken into account by considering the Niño 3 (N3) and Niño 4 (N4) indices, which are the SST averaged, respectively, over El Niño regions 3 (5°N-5°S, 150°-90°W) and 4 (5°N-5°S, 160°E-150°W). Monthly means of N3, N4, N3.4 and SOI were considered here for the period 1875-2016. To interpret low-frequency changes in the ENSO-Paraná flow relationship, we used an index of the Interdecadal Pacific Oscillation (IPO), a slow ENSO-like mode of Pacific climate variability. More specifically, we considered a monthly 1854-2020 record of the tripole IPO index (TPI IPO), which is the difference between the SST anomalies in the equatorial Pacific (10°N-10°S, 170°E-90°W) and those in the Northwest and Southwest Pacific (45°-25°N, 140°E-145°W; 15°-50°S, 150°E-160°W) (Henley et al., 2015).

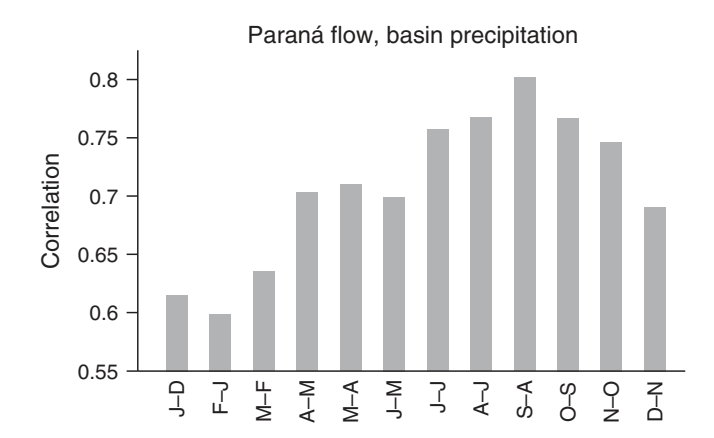


FIGURE 2 Correlation between annual means of Paraná flow at Rosario and basin-integrated precipitation. This correlation was obtained over 1950–2016 and for different definitions of a 12-month year. Letters on the abscissa correspond to month initials. From left to right, the first correlation corresponds to the calendar year January–December (J–D), the second one to the year that starts in February and ends in January of the following year (F–J), and so on. The maximum correlation (0.80) was obtained for the year September–August (S–A). The basin area shown in Figure 1 and the gridded observational rainfall data described in section 2 were used to obtain the basin-integrated precipitation

We also used the following monthly gridded observational data sets: (a) NOAA Extended Reconstructed SST version 5 (NOAA ERSSTv5) data at $2^{\circ} \times 2^{\circ}$ latitude-longitude resolution for 1854–2020 (Huang *et al.*, 2017); (b) Hadley Centre SLP version 2r (HadSLP2r) data at $5^{\circ} \times 5^{\circ}$ resolution for 1850–2019 (Allan and Ansell, 2006); and (c) Global Precipitation Climatology Centre (GPCC) version 2018 rainfall data at $0.5^{\circ} \times 0.5^{\circ}$ resolution for 1950–2016 (Schneider *et al.*, 2018). We did not considered pre-1950 GPCC data because the Paraná-basin pluviometer network was considerably less dense before 1950 than afterwards.

In addition to the above described observational data, we used monthly gridded precipitation estimates from the versions 2c and 3 of the NOAA-CIRES-DOE 20th century reanalysis (20CRv2c and 20CRv3, respectively) (Compo *et al.*, 2011; Slivinski *et al.*, 2019), and from the ECMWF 20th century reanalysis (ERA20C) (Poli *et al.*, 2016). The 20CRv2c, 20CRv3 and ERA20C reanalyses provide, respectively, precipitation data at $2^{\circ} \times 2^{\circ}$, $1^{\circ} \times 1^{\circ}$ and $1.4^{\circ} \times 1.4^{\circ}$ resolution for 1851–2014, 1836–2015 and 1900–2010.

In this study, we considered the hydrological year that starts in September and ends in August of the following year. As shown in Figure 2, this year was identified as the 12-month year that gives the highest correlation between Paraná flow and basin-integrated precipitation. We designate this hydrological year by the calendar year

in which it ends; for example, the year ending in August 2000 is called the 2000 hydrological year. All the results presented in this article were obtained using September–August annual means, with the only exception of those shown in Figure 2. We note that the ENSO mature season (December–February) lies well within the hydrological year considered here (September–August), and thus annual mean flows based on this year definition are suitable for studying the ENSO–Paraná flow link. Another reason for this suitability is the fact that annual averaging filters out subannual flow changes of anthropogenic origin, such as those caused by dam operations (Robertson and Mechoso, 1998).

The zero-lag Pearson correlation coefficient (r) was used in this work to measure the correlation between two time series. To analyse the interdecadal variability of the link between two variables (e.g., Paraná flow and N3.4), we obtained sliding correlation coefficients between them using a 31-year moving window. We chose this window because it encompasses about six full ENSO cycles, and because its length is almost the same as those used in previous studies on long-term changes in the climate responses to ENSO (e.g., McCabe and Dettinger, 1999; Garreaud et al., 2009). The latter facilitates the comparison of the results from our work with those from other studies. We also used a 31-year moving window to calculate the running variance of ENSO indices; this was performed to describe the interdecadal changes in ENSO intensity. Correlation maps between Paraná flow and surface climate variables (SLP and SST) were obtained for different time intervals. These maps allowed us to find the large-scale climate patterns associated with the interannual flow variability observed during particular time periods.

3 | RESULTS AND DISCUSSION

This section presents, discusses and interprets the observed long-term changes in the connectivity between ENSO and Paraná flow. The ability of the state-of-the-art climate reanalyses to reproduce our results is also discussed at the end of this section.

3.1 | Observed changes in ENSO-Paraná flow connectivity

Figure 3a presents the annual mean records of Paraná flow and ENSO indices, and Figure 3b shows the sliding correlation of this flow with these indices. As revealed by the latter (Figure 3b), there were significant positive correlations between Paraná flow and ENSO indices in

1876–1940 and 1983–2016, when large and low flows coincided with El Niño and La Niña episodes, respectively. This Paraná flow response to ENSO is in agreement with that reported in numerous previous studies (e.g., Amarasekera *et al.*, 1997; Camilloni and Barros, 2000; Dettinger and Diaz, 2000; Grimm

et al., 2000; Camilloni and Barros, 2003; Labat et al., 2005; Antico et al., 2014). However, Figure 3b also shows that interannual flow changes were not related to ENSO in 1941–1982, when the sliding correlation of flow with both SOI and N3.4 was not significant (i.e., below the 95% confidence threshold). This ENSO-flow

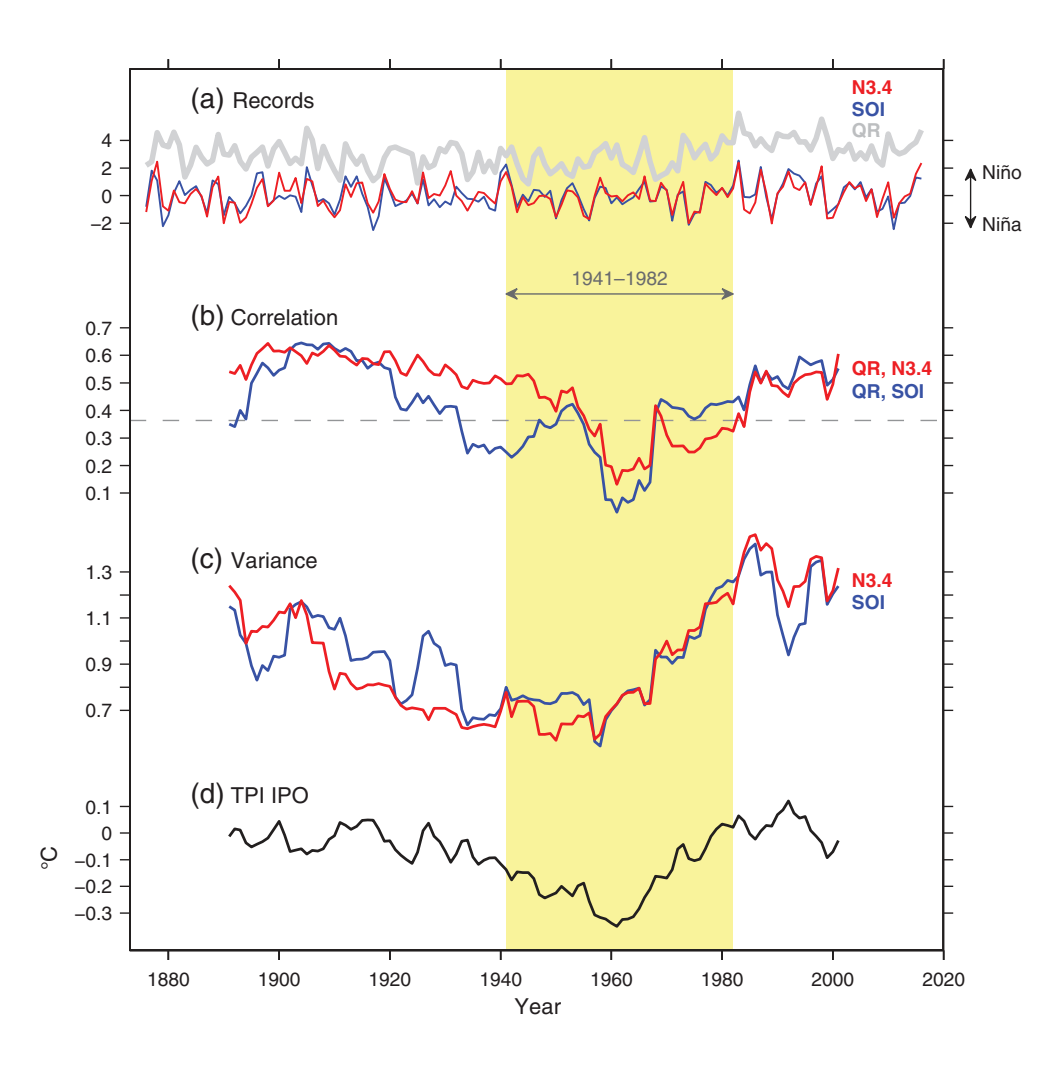


FIGURE 3 (a) Standardized annual mean 1876-2016 records of Paraná flow at Rosario (QR), N3.4, and SOI; to better visualize the records, an offset of 3 was added to QR, and the SOI sign was reversed. (b) Sliding correlation of QR with N3.4 and SOI. (c) Running variance of standardized N3.4 and SOI. (d) Moving average of the tripole IPO index (TPI IPO). In (b-d), a 31-year moving window was used. In (b) the dashed line indicates the upper 95% confidence threshold (2-tailed t test). The shaded area indicates the period 1941-1982, when the correlation of QR with both N3.4 and SOI was below that threshold, that is, when Paraná flow was not connected to ENSO [Colour figure can be viewed at wileyonlinelibrary.com]

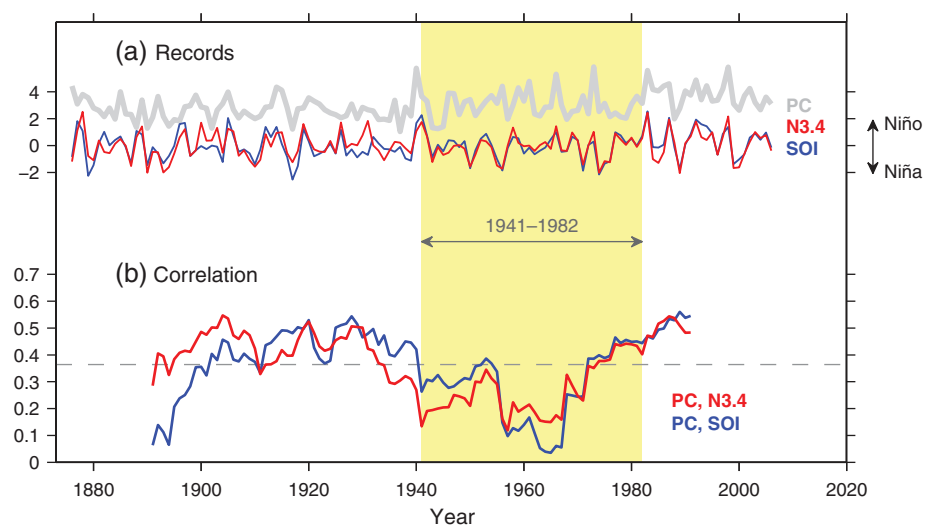


FIGURE 4 Same as Figure 3a,b but for the correlation of the precipitation at Corrientes (PC) with N3.4 and SOI. In (a) the records were standardized and an offset of 3 was added to PC [Colour figure can be viewed at wileyonlinelibrary.com]

disconnection period was also reported, but with less detail, by Labat $et\ al.\ (2005)$ who conducted a cross wavelet analysis of Paraná flow and SOI records over the period 1904–1983. It is interesting to note that the four decades of disconnection in the 20th century explain why some authors (e.g., Amarasekera $et\ al.$, 1997; Antico $et\ al.$, 2014) obtained weak or moderate correlations (r < 0.5) when they correlated ENSO indices and Paraná flow over periods spanning most of the 20th century. But, as shown in Figure 3b, if these variables are correlated

before 1941 or after 1982, then moderate-to-high correlations (r > 0.5) are obtained.

The precipitation record from Corrientes City provides information from a single point location inside the Paraná basin, and thus may not reflect the interannual variability of basin-integrated runoff. Nevertheless, the comparison of Figures 3b and 4 reveals that the interdecadal changes in the correlation of ENSO with Paraná flow are similar to those in the correlation between ENSO and Corrientes precipitation. Hence, this similarity

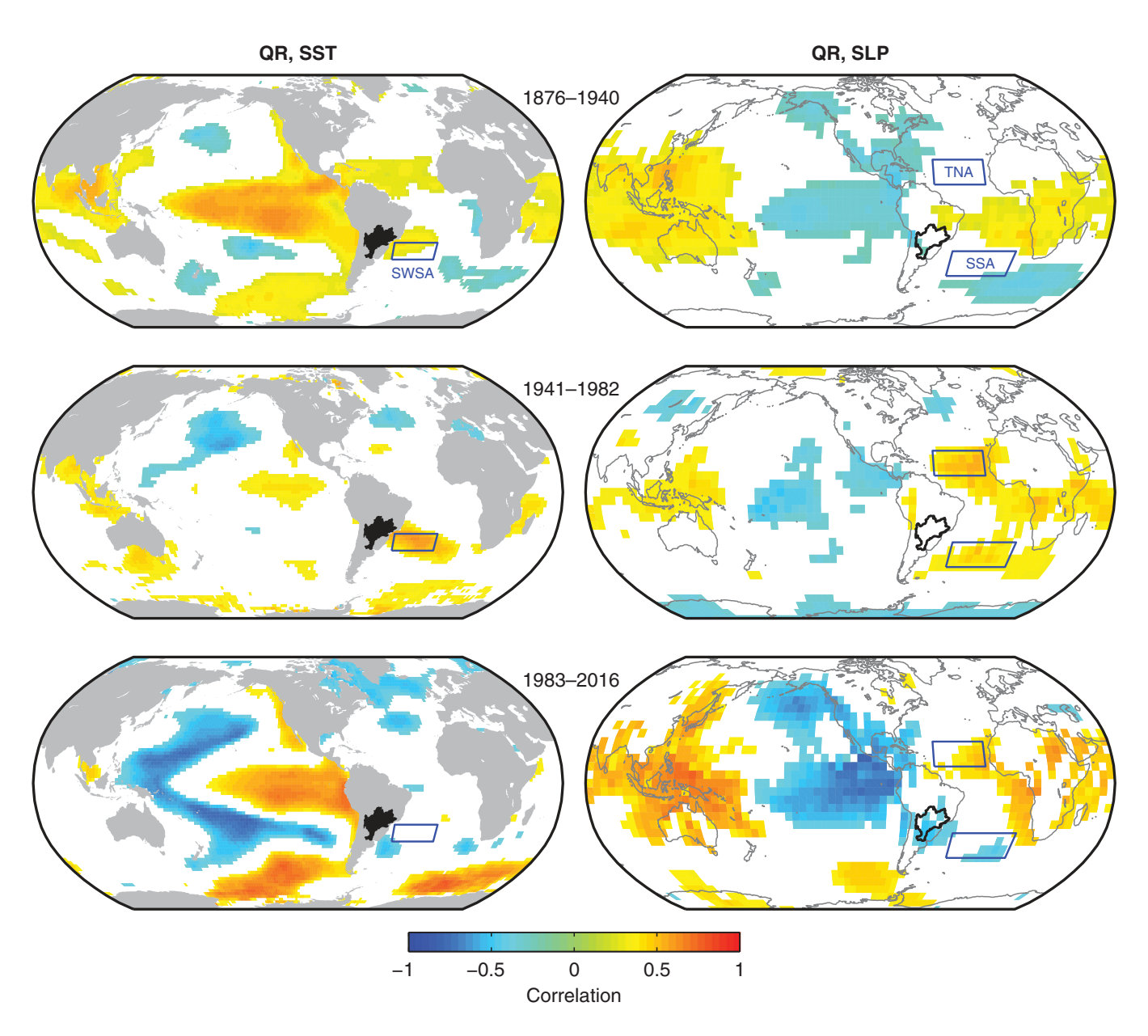


FIGURE 5 Patterns of correlation of Paraná flow at Rosario (QR) with sea surface temperature (SST; left) and sea level pressure (SLP; right) for the periods 1876–1940 (top), 1941–1982 (middle) and 1983–2016 (bottom). Correlation is shown only if significant at the 95% level (2-tailed t test). Sectors considered in this study in the southwestern South Atlantic (SWSA; 25° – 35° S, 45° – 15° W), tropical North Atlantic (TNA; 25° – 10° N, 55° – 20° W) and southern South Atlantic (SSA; 30° – 45° S, 40° W– 5° E) are shown. The Paraná basin is indicated by the black area in left maps and by the thick black line in right maps [Colour figure can be viewed at wileyonlinelibrary.com]

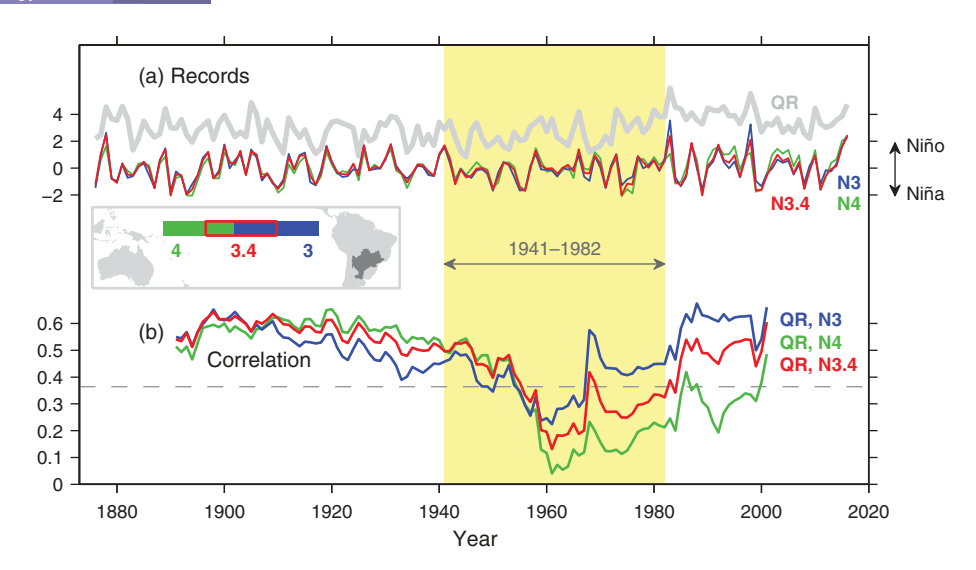


FIGURE 6 Same as Figure 3a,b but for the correlation of Paraná flow at Rosario (QR) with the N3, N4 and N3.4 indices, which are the sea surface temperature averaged respectively over El Niño regions 3 (5° N- 5° S, 150° - 90° W), 4 (5° N- 5° S, 160° E- 150° W) and 3.4 (5° N- 5° S, 170° - 120° W). The inset map shows the location of these regions (rectangles) and that of the Paraná basin (dark grey area). In (a) the records were standardized and an offset of 3 was added to QR. In (b) the dashed line indicates the upper 95% confidence threshold (2-tailed *t* test) [Colour figure can be viewed at wileyonlinelibrary.com]

lends further support to the observed long-term changes in the ENSO-Paraná flow link. We also note that, as expected, the interdecadal variations of ENSO-Corrientes rainfall correlation shown in Figure 4 are similar to those shown by Garreaud *et al.* (2009). But they are not identical because, while we averaged variables over the hydrological year September-August, Garreaud *et al.* (2009) considered October-December averages of SOI and Corrientes precipitation.

It is also worth mentioning that, since 1875, the most devastating Paraná floods occurred in the hydrological years 1878, 1905, 1983, 1992 and 1998, when strong El Niño events developed (Antico *et al.*, 2016; 2020; Antico and Diaz, 2020). That is, none of these extreme floods occurred during 1941–1982, when there was no relationship between ENSO and Paraná flow. This is consistent with previous studies that indicated an important role of ENSO in the generation of extreme Paraná floods (e.g., Grimm *et al.*, 2000; Camilloni and Barros, 2003; Antico *et al.*, 2016; Antico and Diaz, 2020).

3.2 | SST and SLP patterns associated with periods of connection and disconnection

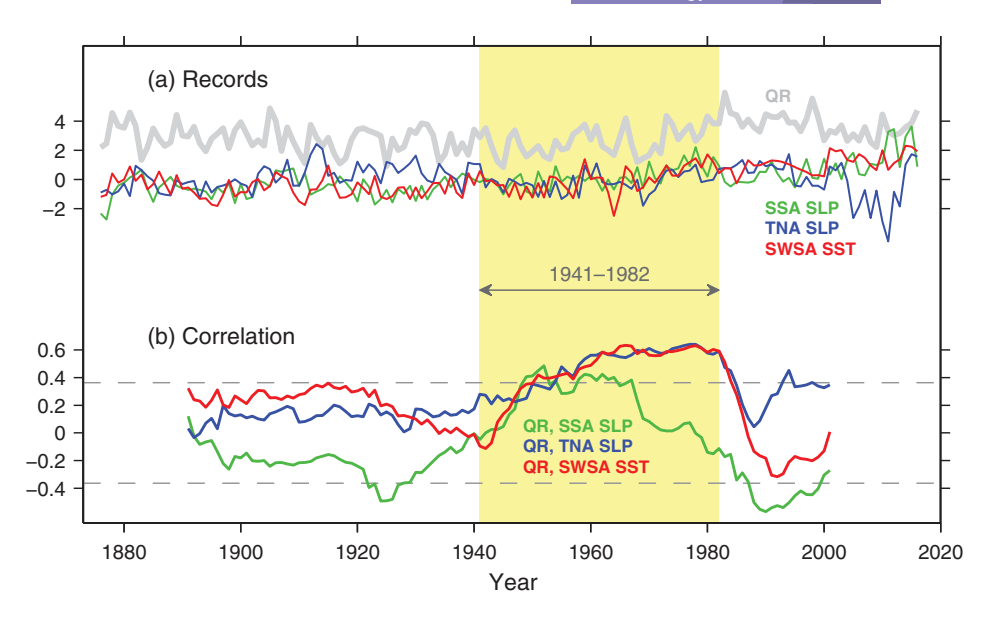
Top and bottom maps of Figure 5 show the large-scale SST and SLP patterns that were associated with Paraná flow variability during the two periods of significant ENSO-flow connection (1876–1940 and 1983–2016). As expected, these SST and SLP patterns are those characteristic of ENSO.

Given that these patterns are widely described and discussed in the literature (see the review by Cai et al., 2020), they are not discussed here. We only make the following two comments about them. First, the significant SST-flow correlation observed in the Pacific sector of the Southern Ocean in 1876-1940 and 1983-2016 (see left top and left bottom of Figure 5) probably reflects the ENSO teleconnection to the Southern Ocean (Yuan Martinson, 2000; Kwok and Comiso, 2002), rather than a direct influence of this ocean on the Paraná flow. Second, the region of strongest SST-flow correlation changed its location from the central equatorial Pacific in 1876–1940 to a more eastern location in 1983–2016 (compare left top and left bottom maps of Figure 5). This is corroborated by the results shown in Figure 6, where it can be seen that the Paraná flow variability was generally more correlated with central equatorial Pacific SST changes (described by N4) before 1941, but notably more correlated with eastern equatorial Pacific SST (depicted by N3) after 1982. Such an eastward shift of the maximum SST-flow correlation region could imply a change in the ENSO-Paraná basin teleconnection pattern (Sulca et al., 2018).

For the period when the relationship between Paraná flow and ENSO was weak and not significant (1941–1982), the middle maps of Figure 5 present the patterns of correlation of flow with SST and SLP. While the SST pattern shows a significant positive SST–flow correlation in a sector of the southwestern South Atlantic (SWSA), the SLP pattern reveals a significant positive SLP–flow correlation in sectors of the tropical North Atlantic (TNA) and southern South Atlantic (SSA)

RMetS

FIGURE 7 Same as Figure 3a,b but for the correlation of Paraná flow at Rosario (QR) with sea surface temperature (SST) averaged over the southwestern South Atlantic (SWSA) sector, and with sea level pressure (SLP) averaged over the tropical North Atlantic (TNA) and southern South Atlantic (SSA) sectors. These three Atlantic sectors (SWSA, TNA and SSA) are indicated in Figure 5. In (a) the records were standardized and an offset of 3 was added to QR. In (b) the dashed lines indicate the 95% confidence thresholds (2-tailed t test) [Colour figure can be viewed at wileyonlinelibrary.com



Oceans. To further investigate these correlations, we calculated the sliding correlation of Paraná flow with SST averaged over the SWSA sector, and with SLP averaged over the TNA and SSA sectors. As shown in Figure 7, the obtained moving correlations confirm that a significant relationship between Paraná flow and climate variability in the SWSA, TNA and SSA sectors existed in 1941-1982, when this river flow was not related to ENSO. Interestingly, Figure 7 also reveals that in these years the correlation of Paraná flow with SWSA SST and with TNA SLP was stronger and more persistent than that with SSA SLP. This suggests that in 1941–1982 the Paraná flow variability was more influenced by TNA SLP and SWSA SST changes than by the SSA SLP variability. In line with this, it is noteworthy that previous observational and numerical studies identified a link between southeastern South American rainfall and SWSA SST (Barros et al., 2000; Grimm and Zilli, 2009; Bombardi et al., 2014; Cherchi et al., 2014). According to these studies, warmer (colder) SWSA SSTs are accompanied by a southward (northward) displacement of the South Atlantic Convergence Zone, and this shift is in turn associated with enhanced (diminished) Paraná basin rainfall.

3.3 | Possible causes of changes in ENSO-Paraná flow connectivity

The ENSO-related Pacific SST and SLP changes can be described as anomalies or departures from a background mean state (Fedorov and Philander, 2000). This mean state and the amplitude of these anomalies both exhibit interdecadal fluctuations that can drive long-term changes in the teleconnections of ENSO to the climate of

a particular region (Diaz *et al.*, 2001). As explained below, this seems to be the case for the Paraná basin.

Figure 3b,c reveals that ENSO anomalies of Pacific SST and SLP (i.e., N3.4 and SOI changes, respectively) reached their lowest insignificant correlation with Paraná flow around 1960, approximately at the time when they also reached their lowest variances (squared amplitudes). Hence, the ENSO teleconnection to Paraná flow appears to vanish when these Pacific ENSO anomalies are too small to exert a noticeable influence on the Paraná basin climate. Conversely, an ENSO-Paraná flow relationship seems to exist when these anomalies become larger (see Figure 3b,c). This behaviour is consistent with numerical climate simulations whose results show that the ENSO influence on Pacific-North American climate becomes stronger as the tropical ENSO SST anomalies get larger (Kumar and Hoerling, 1998).

Since the ENSO teleconnections are ultimately determined by the absolute values of equatorial Pacific SSTs, a change in the background state of these SSTs can alter the teleconnections, even if there is no change in the amplitude of the SST anomalies that fluctuate around the mean state (Diaz et al., 2001). Thus, because lowfrequency changes of the background equatorial Pacific SST follow those of the IPO, it seems sensible to investigate whether or not this Pacific multidecadal mode of variability is related to the observed changes in the ENSO-Paraná flow connection. Figure 3b,d reveals that when this connection disappeared in 1941-1982, the IPO TPI did indeed reach its most negative values. This suggests that the ENSO teleconnection to Paraná flow vanishes during very cold IPO phases. Interestingly, such an IPO modulation of ENSO influences on climate was also found in other regions such as the western United States, northeastern Australia, northern India and southern Africa

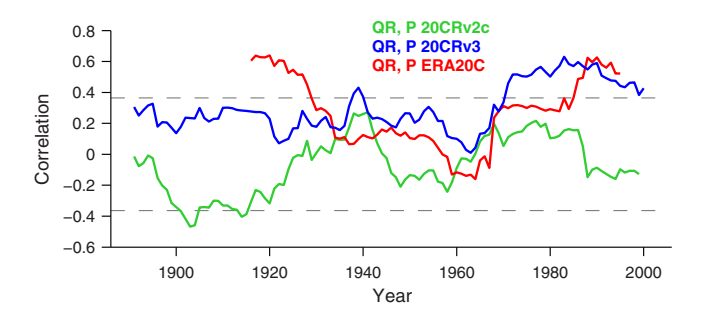


FIGURE 8 Sliding correlation (31-year window) of Paraná flow observed at Rosario (QR) with basin-integrated precipitation (P) from three long-term climate reanalyses (20CRv2c, 20CRv3 and ERA20C; see section 2 for details on these reanalyses). Dashed lines indicate the 95% confidence thresholds (2-tailed *t* test) [Colour figure can be viewed at wileyonlinelibrary.com]

(McCabe and Dettinger, 1999; Power *et al.*, 1999; Dong and Dai, 2015). However, in contrast to the Paraná basin, some of these other regions (e.g., western United States and northeastern Australia) experienced a weakened or no ENSO-climate connection during warm IPO phases. That is, as shown by Dong and Dai (2015), the IPO modulation appears to operate differently in different regions. Furthermore, in a given region this modulation can be asymmetric with respect to ENSO and IPO phases (Dong *et al.*, 2018). For instance, the IPO can modulate El Niño effects differently than La Niña effects. Future proxy and modelling studies could investigate the existence of such asymmetric IPO modulation in the Paraná basin.

3.4 | Are climate reanalyses suitable to study changes in ENSO-Paraná flow connectivity?

Twentieth-century reanalysis products spanning the last 100 years or more would be ideally suited to diagnose the mechanisms that can explain the above described long-term changes in ENSO-Paraná flow connectivity. However, the state-of-the-art climate reanalyses do not satisfactorily reproduce the interannual variability of precipitation integrated over the Paraná basin. In the case of the NOAA 20CRv2c reanalysis, the diagnosed basin-integrated rainfall was never significantly and positively correlated with the observed Paraná flow (see Figure 8). Basin precipitation from the ERA20C reanalysis is realistic but only for the years before 1930 and after 1985 (Figure 8). The rainfall from the NOAA 20CRv3 reanalysis has been in reasonable agreement with the observed flow, but only since 1970 (Figure 8). This probably reflects the relatively low number of pre-1970 meteorological observations assimilated into the reanalysis system. Thus, the agreement between the

observed Paraná flow and rainfall from reanalyses could be improved by future work aimed at assimilating more pre-1970 observations into the reanalyses. Future improvements of reanalysis numerical models could also increase this agreement, not only before 1970, but also after this year. In the meantime, the limited agreement reported here highlights the need and usefulness of conducting observation-based studies like the one presented here.

4 | CONCLUSIONS

We have revealed in detail the long-term changes in the connectivity between ENSO and the flow of the Paraná, one of the world's largest rivers. To do this, we employed a recently rescued 1876–2016 record of Paraná flow in conjunction with other observational climate datasets. Our main conclusions are the following:

- 1. ENSO significantly influenced Paraná flow in 1876–1940 and 1983–2016, but not during the period 1941–1982.
- 2. Paraná flow variability was more related to central Pacific ENSO SST fluctuations before 1941, but more linked with eastern Pacific SST after 1982. That is, the region of strongest SST-flow correlation changed its location from the central equatorial Pacific in 1876– 1940 to a more eastern location in 1983–2016. This result suggests a change in the ENSO-Paraná basin teleconnection pattern.
- 3. From 1941 to 1982, the interannual variability of Paraná flow was positively correlated with SST in the southwestern South Atlantic Ocean, and with SLP in the tropical North Atlantic and southern South Atlantic Oceans. That is, Atlantic climate variability may have notably influenced the Paraná flow variability at a time when ENSO had no effect on this river flow.
- 4. ENSO-related Pacific climate anomalies reached their lowest insignificant correlation with Paraná flow around 1960, approximately at the same time as when they also reached their lowest amplitudes. A possible explanation for this observation is that the Paraná flow becomes disconnected from ENSO when this climate mode is too weak to exert a significant influence on Paraná basin precipitation.
- 5. The ENSO-Paraná flow relationship disappeared during the coldest IPO phase of the study period. Hence, the IPO may be modulating the ENSO effect on Paraná flow in a manner that disables this teleconnection during very cold IPO phases. This in turn suggests that the IPO may determine during which decades ENSO indices (e.g., SOI) can serve as useful predictors for Paraná flow.



6. Twentieth-century climate reanalyses do not successfully reproduce the observed Paraná basin rainfall and, thus, cannot aid in the interpretation of our results. This problem might be overcome by future reanalysis improvements, such as the assimilation of more historical (pre-1970) meteorological observations into the reanalyses.

Finally, we emphasize that although we notably improved the description and interpretation of decadal changes in the ENSO-Paraná flow connectivity, we did not focus on the physical mechanisms that underlie these changes. Nonetheless, we offer our observation-based results as valuable diagnostic information for future modelling studies aimed at elucidating these mechanisms.

ACKNOWLEDGEMENTS

Mathias Vuille was partially supported by US-NSF award OISE-1743738. The Paraná flow data used in this study are available at the Pangaea database (https://doi.pangaea.de/10.1594/PANGAEA.882613, https://doi.pangaea. de/10.1594/PANGAEA.906056). GPCC gridded data were provided by the German National Meteorological Service (data available at https://www.dwd.de/). Corrientes City precipitation data were obtained from the NOAA/NCEI web site (https://www.ncei.noaa.gov/). The following datasets were downloaded from the web site of the NOAA PSL (https://psl.noaa.gov/): Niño 3, Niño 4, Niño 3.4 and SOI records; unfiltered TPI IPO values from ERSSTv5 data; HadSLP2r and ERSSTv5 gridded data; NOAA-CIRES-DOE 20CRv2c and 20CRv3 reanalysis data. ECMWF ERA20C reanalysis data were obtained from the KNMI Climate Explorer (https://climexp.knmi. nl/). The authors would like to thank Henry F. Diaz and two anonymous reviewers for their constructive comments that improved the manuscript.

AUTHOR CONTRIBUTIONS

Andrés Antico: Conceptualization; formal analysis; investigation; methodology; resources; visualization; writing – original draft; writing – review and editing. **Mathias Vuille:** Formal analysis; investigation; methodology; resources; writing – original draft; writing – review and editing.

CONFLICT OF INTEREST

The authors declare no potential conflict of interest.

ORCID

Andrés Antico https://orcid.org/0000-0003-2985-9620

Mathias Vuille https://orcid.org/0000-0002-9736-4518

REFERENCES

- Abou Rafee, S.A., Uvo, C.B., Martins, J.A., Machado, C.B. and Freitas, E.D. (2022) Land use and cover changes versus climate shift: Who is the main player in river discharge? A case study in the Upper Paraná River basin. *Journal of Environmental Management*, 309, 114651.
- Allan, R. and Ansell, T. (2006) A new globally complete monthly historical gridded mean sea level pressure dataset (HadSLP2): 1850–2004. *Journal of Climate*, 19, 5816–5842.
- Amarasekera, K.N., Lee, R.F., Williams, E.R. and Eltahir, E.A.B. (1997) ENSO and the natural variability in the flow of tropical rivers. *Journal of Hydrology*, 200, 24–39.
- Anderson, R.J., da Franca Ribeiro dos Santos, N. and Diaz, H.F. (1993) *An analysis of flooding in the Paraná/Paraguay River basin*. Washington D.C.: World Bank. LATEN Dissemination Note No. 5.
- Antico, A., Aguiar, R.O. and Amsler, M.L. (2018) Hydrometric data rescue in the Paraná River basin. Water Resources Research, 54, 1368–1381.
- Antico, A. and Diaz, H.F. (2020) Why was the Paraná flood of 2016 weaker than that of 1998? *International Journal of Climatology*, 40, 604–609.
- Antico, A., Mendizabal, S., Ferreira, L.J., Aguiar, R.O. and Amsler, M.L. (2020) Addendum to "Hydrometric data rescue in the Paraná River basin" by Andrés Antico, Ricardo O. Aguiar, and Mario L. Amsler. Water Resources Research, 56, e2019WR026654.
- Antico, A., Schlotthauer, G. and Torres, M.E. (2014) Analysis of hydroclimatic variability and trends using a novel empirical mode decomposition: application to the Paraná River basin. *Journal of Geophysical Research: Atmospheres*, 119, 1218– 1233.
- Antico, A., Torres, M.E. and Diaz, H. (2016) Contributions of different time scales to extreme Paraná floods. *Climate Dynamics*, 46, 3785–3792.
- Barros, V., Gonzalez, M., Liebmann, B. and Camilloni, I. (2000) Influence of the South Atlantic convergence zone and South Atlantic Sea surface temperature on interannual summer rainfall variability in southeastern South America. *Theoretical and Applied Climatology*, 67, 123–133.
- Bombardi, R.J., Carvalho, L.M.V., Jones, C. and Reboita, M.S. (2014) Precipitation over eastern South America and the South Atlantic Sea surface temperature during neutral ENSO periods. Climate Dynamics, 42, 1553–1568.
- Cai, W., McPhaden, M., Grimm, A., Rodrigues, R.R., Garreaud, R. D., Dewitte, B., Poveda, G., Ham, Y., Santoso, A., Ng, B., Anderson, W., Wang, G., Geng, T., Jo, H., Marengo, J.A., Alves, L.M., Osman, M., Li, S., Wu, L., Karamperidou, C., Takahashi, K. and Vera, C. (2020) Climate impacts of the El Niño–Southern Oscillation on South America. *Nature Reviews Earth & Environment*, 1, 215–231.
- Camilloni, I.A. and Barros, V.R. (2000) The Paraná River response to El Niño 1982–83 and 1997–98 events. *Journal of Hydrometeorology*, 1, 412–430.
- Camilloni, I.A. and Barros, V.R. (2003) Extreme discharge events in the Paraná River and their climate forcing. *Journal of Hydrology*, 278, 94–106.
- Cherchi, A., Carril, A.F., Menéndez, C.G. and Zamboni, L. (2014) La Plata basin precipitation variability in spring: role of remote

- SST forcing as simulated by GCM experiments. *Climate Dynamics*, 42, 219–236.
- Compo, G.P., Whitaker, J.S., Sardeshmukh, p.D., Matsui, N., Allan, R.J., Yin, X., Gleason, B.E., Vose, R.S., Rutledge, G., Bessemoulin, P., Brönnimann, S., Brunet, M., Crouthamel, R.I., Grant, A.N., Groisman, p.Y., Jones, p.D., Kruk, M.C., Kruger, A. C., Marshall, G.J., Maugeri, M., Mok, H.Y., Nordli, Ø., Ross, T. F., Trigo, R.M., Wang, X.L., Woodruff, S.D. and Worley, S.J. (2011) The twentieth century reanalysis project. *Quarterly Journal of the Royal Meteorological Society*, 137, 1–28.
- Dettinger, M.D. and Diaz, H.F. (2000) Global characteristics of stream flow seasonality and variability. *Journal of Hydrometeo-rology*, 1, 289–310.
- Diaz, H.F., Hoerling, M.P. and Eischeid, J.K. (2001) ENSO variability, teleconnections and climate change. *International Journal of Climatology*, 21, 1845–1862.
- Dong, B. and Dai, A. (2015) The influence of the Interdecadal Pacific Oscillation on temperature and precipitation over the globe. Climate Dynamics, 45, 2667–2681.
- Dong, B., Dai, A., Vuille, M. and Timm, O.E. (2018) Asymmetric modulation of ENSO teleconnections by the Interdecadal Pacific Oscillation. *Journal of Climate*, 31, 7337–7361.
- Fedorov, A.V. and Philander, S.G. (2000) Is El Niño changing? *Science*, 288, 1997–2002.
- Garreaud, R.D., Vuille, M., Compagnucci, R. and Marengo, J. (2009) Present-day South American climate. *Palaeogeography Palaeoclimatology Palaeoecology*, 281, 180–195.
- GRDC (2020) Major river basins of the World/Global Runoff Data Centre (GRDC), 2nd edition. Koblenz: Federal Institute of Hydrology (BfG). Technical report.
- Grimm, A.M., Barros, V.R. and Doyle, M.E. (2000) Climate variability in southern South America associated with El Niño and La Niña events. *Journal of Climate*, 13, 35–58.
- Grimm, A.M. and Zilli, M.T. (2009) Interannual variability and seasonal evolution of summer monsoon rainfall in South America. *Journal of Climate*, 22, 2257–2275.
- Henley, B.J., Gergis, J., Karoly, D.J., Power, S., Kennedy, J. and Folland, C.K. (2015) A Tripole Index for the Interdecadal Pacific Oscillation. *Climate Dynamics*, 45, 3077–3090.
- Huang, B., Thorne, p.W., Banzon, V.F., Boyer, T., Chepurin, G., Lawrimore, J.H., Menne, M.J., Smith, T.M., Vose, R.S. and Zhang, H. (2017) Extended Reconstructed Sea Surface Temperature, version 5 (ERSSTv5): upgrades, validations, and intercomparisons. *Journal of Climate*, 30, 8179–8205.
- Kumar, A. and Hoerling, M.P. (1998) Annual cycle of Pacific–North American seasonal predictability associated with different phases of ENSO. *Journal of Climate*, 11, 3295–3308.
- Kwok, R. and Comiso, J.C. (2002) Southern Ocean climate and sea ice anomalies associated with the Southern Oscillation. *Journal* of Climate, 15, 487–501.
- Labat, D., Ronchail, J. and Guyot, J.L. (2005) Recent advances in wavelet analyses: part 2—Amazon, Parana, Orinoco and Congo discharges time scale variability. *Journal of Hydrology*, 314, 289–311.
- Lee, E., Livino, A., Han, S., Zhang, K., Briscoe, J., Kelman, J. and Moorcroft, P. (2018) Land cover change explains the increasing discharge of the Paraná River. *Regional Environmental Change*, 18, 1871–1881.

- McCabe, G.J. and Dettinger, M.D. (1999) Decadal variations in the strength of ENSO teleconnections with precipitation in the western United States. *International Journal of Climatology*, 19, 1399–1410.
- Montroull, N.B., Saurral, R.I. and Camilloni, I.A. (2018) Hydrological impacts in La Plata basin under 1.5, 2 and 3 °C global warming above the pre-industrial level. *International Journal of Climatology*, 38, 3355–3368.
- Pasquini, A.I. and Depetris, p.J. (2010) ENSO-triggered exceptional flooding in the Paraná River: Where is the excess water coming from? *Journal of Hydrology*, 383, 186–193.
- Poli, P., Hersbach, H., Dee, D.P., Berrisford, P., Simmons, A.J., Vitart, F., Laloyaux, P., Tan, D.G.H., Peubey, C., Thépaut, J., Trémolet, Y., Hólm, E.V., Bonavita, M., Isaksen, L. and Fisher, M. (2016) ERA-20C: an atmospheric reanalysis of the twentieth century. *Journal of Climate*, 29, 4083–4097.
- Power, S., Casey, T., Folland, C., Colman, A. and Mehta, V. (1999) Inter-decadal modulation of the impact of ENSO on Australia. *Climate Dynamics*, 15, 319–324.
- Robertson, A.W. and Mechoso, C.R. (1998) Interannual and decadal cycles in river flows of southeastern South America. *Journal of Climate*, 11, 2570–2581.
- Schneider, U., Becker, A., Finger, P., Meyer-Christoffer, A. and Ziese, M. (2018) GPCC full data monthly product version 2018 at 0.5°: monthly land-surface precipitation from raingauges built on GTS-based and historical data. Offenbach am Main, Germany: Global Precipitation Climatology Centre. Technical report.
- Schumm, S.A. and Winkley, B.R. (1994) The character of large alluvial rivers. In: Schumm, S.A. and Winkley, B.R. (Eds.) *The Variability of Large Alluvial Rivers*. New York, NY: American Society of Civil Engineers, pp. 1–9.
- Silva, C.B., Silva, M.E.S. and Ambrizzi, T. (2017) Climatic variability of river outflow in the Pantanal region and the influence of sea surface temperature. *Theoretical and Applied Climatology*, 129, 97–109.
- Slivinski, L.C., Compo, G.P., Whitaker, J.S., Sardeshmukh, p.D., Giese, B.S., McColl, C., Allan, R., Yin, X., Vose, R., Titchner, H., Kennedy, J., Spencer, L.J., Ashcroft, L., Brönnimann, S., Brunet, M., Camuffo, D., Cornes, R., Cram, T. A., Crouthamel, R., Domínguez-Castro, F., Freeman, J.E., Gergis, J., Hawkins, E., Jones, p.D., Jourdain, S., Kaplan, A., Kubota, H., Blancq, F.L., Lee, T., Lorrey, A., Luterbacher, J., Maugeri, M., Mock, C.J., Moore, G.W.K., Przybylak, R., Pudmenzky, C., Reason, C., Slonosky, V.C., Smith, C.A., Tinz, B., Trewin, B., Valente, M.A., Wang, X.L., Wilkinson, C., Wood, K. and Wyszyński, P. (2019) Towards a more reliable historical reanalysis: improvements for version 3 of the twentieth century reanalysis system. *Quarterly Journal of the Royal Meteorological Society*, 145, 2876–2908.
- Sulca, J., Takahashi, K., Espinoza, J., Vuille, M. and Lavado-Casimiro, W. (2018) Impacts of different ENSO flavors and tropical Pacific convection variability (ITCZ, SPCZ) on austral summer rainfall in South America, with a focus on Peru. *International Journal of Climatology*, 38, 420–435.
- UNESCO (2007) La Plata basin case study: final report. Perugia, Italy: UNESCO World Water Assessment Programme. Report UN-WATER/WWAP/2007/03.

Vose, R. S., Schmoyer, R. L., Steurer, P. M., Peterson, T. C., Heim, R., Karl, T. R. and Eischeid, J. K. (1992) The global historical climatology network: long-term monthly temperature, precipitation, sea level pressure, and station pressure data. Oak Ridge, TN Carbon Dioxide Information Analysis Center, Oak Ridge National Laboratory. Technical report.

Yuan, X. and Martinson, D.G. (2000) Antarctic Sea ice extent variability and its global connectivity. *Journal of Climate*, 13, 1697–1717.

How to cite this article: Antico, A., & Vuille, M. (2022). ENSO and Paraná flow variability: Long-term changes in their connectivity. International Journal of Climatology, 1–11. https://doi.org/10.1002/joc.7643